

# Flux qubit as a sensor for a magnetometer with quantum limited sensitivity

E. Il'ichev<sup>1,\*</sup> and Ya. S. Greenberg<sup>2</sup>

<sup>1</sup>*Institute for Physical High Technology, P.O. Box 100239, D-07702 Jena, Germany*

<sup>2</sup>*Novosibirsk State Technical University, 20 K. Marx Ave., 630092 Novosibirsk, Russia.*

(Dated: October 24, 2018)

We propose to use the quantum properties of a superconducting flux qubit in the construction of a magnetometer with quantum limited sensitivity. The main advantage of a flux qubit is that its noise is rather low, and its transfer functions relative to the measured flux can be made to be about  $10\text{mV}/\Phi_0$ , which is an order of magnitude more than the best value for a conventional SQUID magnetometer. We analyze here the voltage-to-flux, the phase-to-flux transfer functions and the main noise sources. We show that the experimental characteristics of a flux qubit, obtained in recent experiments, allow the use of a flux qubit as magnetometer with energy resolution close to the Planck constant.

PACS numbers: 74.50.+r, 84.37.+q, 03.67.-a

Josephson-junction qubits are known to be candidates for solid-state quantum computing circuits<sup>1</sup>. However, owing to their unique quantum properties these devices undoubtedly can be used as sensitive detectors of different physical quantities, such as quantum environmental noise<sup>2</sup> or low frequency fluctuations of the junction critical current<sup>3</sup>. Here we propose to use a Josephson-junction flux qubit as a sensitive detector of magnetic flux<sup>4</sup>. We show that the present state-of-art allows one to obtain the energy sensitivity of such a detector in the order of the Planck constant.

A flux qubit<sup>5,6,7</sup> consists of three Josephson junctions in a loop with very small inductance  $L$ , typically in the pH range. This ensures an effective decoupling from the environment. Two junctions have an equal critical current  $I_c$  and (effective) capacitance  $C$ , while those of the third junction are slightly smaller:  $\alpha I_c$  and  $\alpha C$ , with  $0.5 < \alpha < 1$ . At sufficiently low temperatures (typically  $T \approx (10 \sim 30)$  mK) when  $\Phi_x$ , the external flux applied to the qubit loop, is in the close vicinity of  $\Phi_0/2$  ( $\Phi_0 = h/2e$  is the flux quantum,  $h$  is the Planck constant) the system has two low-lying quantum states  $E_-$  and  $E_+$ . The energy gap of the flux qubits,  $\Delta/h = (E_+ - E_-)/h$  is of the order of several GHz. Below we assume  $k_B T \ll \Delta$  ( $k_B$  is the Boltzmann constant), so that the qubit is definitely in its ground state  $E_-$ <sup>8</sup>.

For experimental characterization the flux qubit is inductively coupled through a mutual inductance  $M$  to an  $LC$  tank circuit with known inductance  $L_T$ , capacitance  $C_T$ , and quality  $Q$  (Fig. 1).

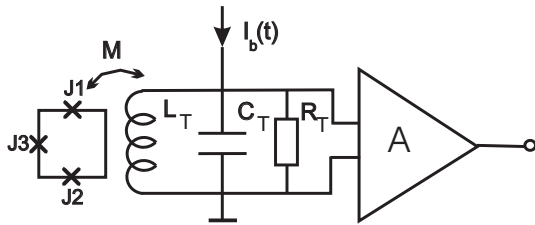


FIG. 1: Flux qubit coupled to a tank.

The resonant characteristics of the tank circuit (frequency, phase shift, etc.) are sensitive to the qubit inductance and therefore to the external flux  $\Phi_x$ .

It was shown in<sup>9</sup> that the amplitude  $v$  and the phase  $\chi$  of the output signal  $V(t) = v \cos(\omega t + \chi)$  are coupled by the equations:

$$v^2 (1 + 4Q^2 \xi^2(f_x)) = I_0^2 \omega_T^2 L_T^2 Q^2 \quad (1)$$

$$\tan \chi = 2Q \xi(f_x), \quad (2)$$

where  $I_0$  is the amplitude of the driving current ( $I_b(t) = I_0 \cos \omega t$ ), and  $\omega$  and  $\omega_T$  are a driving frequency and the resonant frequency of the tank circuit, respectively.

It is worth noting that the the scheme in Fig. 1 and Eqs. (1), (2) are quite similar to those for a conventional RF SQUID. The only difference is in the expression for a flux-dependent frequency detuning  $\xi(f_x)$ . This depends on the qubit parameters as<sup>9</sup>:

$$\xi(f_x) = \xi_0 - k^2 \frac{L I_c^2}{\Delta} \left( \frac{\lambda}{2\pi} \right)^2 F(f_x), \quad (3)$$

$$\xi_0 = (\omega_T - \omega)/\omega_T, \quad f_x = \Phi_x/\Phi_0 - \frac{1}{2}, \quad \text{and}$$

$$F(f_x) = \frac{1}{\pi} \int_0^{2\pi} d\phi \frac{\cos^2 \phi}{[1 + \eta^2 (f_x + \gamma \sin \phi)^2]^{3/2}}, \quad (4)$$

with  $\eta = 2E_J \lambda / \Delta$  and  $\gamma = M I_0 Q / \Phi_0$ . The expression for  $\lambda$ , which depends on  $\alpha$ ,  $I_c$  and  $C$  is given in<sup>9</sup>.

Therefore, the main effect of the qubit-tank interaction is a shift of the tank resonance. This results in a dip in the voltage-to-flux and phase-to-flux characteristics which have been confirmed by experiments<sup>10</sup>.

Theoretical phase-to-flux  $\chi(f_x)$  (PFC) and voltage-to-flux (VFC)  $v(f_x)$  dependencies at resonance  $\omega = \omega_T$ , are shown in Fig. 2 for three values of the amplitude of the bias current  $I_0$ . The graphs have been calculated from

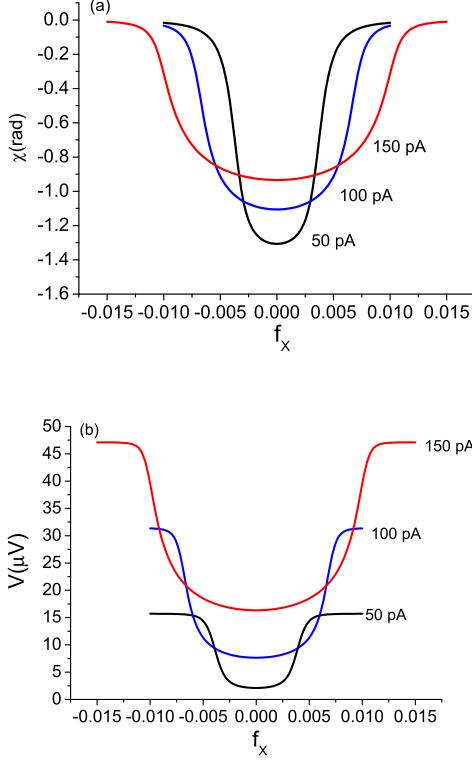


FIG. 2: (Color online). Tank phase  $\chi$  (a) and tank voltage  $V$  (b) vs bias flux  $f_x$  for three values of bias current  $I_0$ . The gap frequency  $\Delta/h = 2\text{GHz}$ .

Eqs.(1), (2) for the following qubit-tank parameters:  $I_c = 400\text{ nA}$ ,  $\alpha = 0.8$ ,  $L = 40\text{ pH}$ ,  $L_T = 50\text{ nH}$ ,  $Q = 10000$ ,  $\omega_T/2\pi = 100\text{ MHz}$ ,  $\Delta/h = 2\text{GHz}$ , and  $k = 10^{-2}$ .

The advantage of a qubit magnetometer over a conventional SQUID magnetometer is in the very steep dependence of its VFC and PFC. In the flux locked loop operation of a magnetometer the working point is set at a fixed value of  $\Phi_X$  where the slope of VFC or PFC is maximum. The output signal  $\delta V$  is proportional to the change  $\delta\Phi_X$  of the measured flux. In principle two modes of detection are possible: voltage mode, where  $\delta V = V_\Phi \delta\Phi_X$ , and the phase mode, where  $\delta V = \chi_\Phi \delta\Phi_X$ . The qubit transfer functions  $\chi_\Phi = v\partial\chi/\partial\Phi_X$  and  $V_\Phi = \partial v/\partial\Phi_X$  are shown in Fig. 3 for the same qubit-tank parameters as those used in Fig. 2. It is seen that qubit transfer functions can exceed  $10\text{ mV}/\Phi_0$ . This value should be compared with  $1\text{ mV}/\Phi_0$ , the best value obtained for a DC SQUID with additional positive feedback<sup>12</sup>.

The flux and energy sensitivity depend on the main noise sources, which come from the low frequency fluctuations of the junction critical current,  $S_{I_c}$ , and from the voltage noise,  $S_V$  and the current noise,  $S_I$  of the preamplifier, where  $S_{I_c}$ ,  $S_V$  and  $S_I$  are the corresponding spectral densities. The fluctuations of  $I_c$  result in the fluctuating flux in the qubit loop  $S_{\Phi, I_c}^{1/2} = LS_{I_c}^{1/2}$ . For

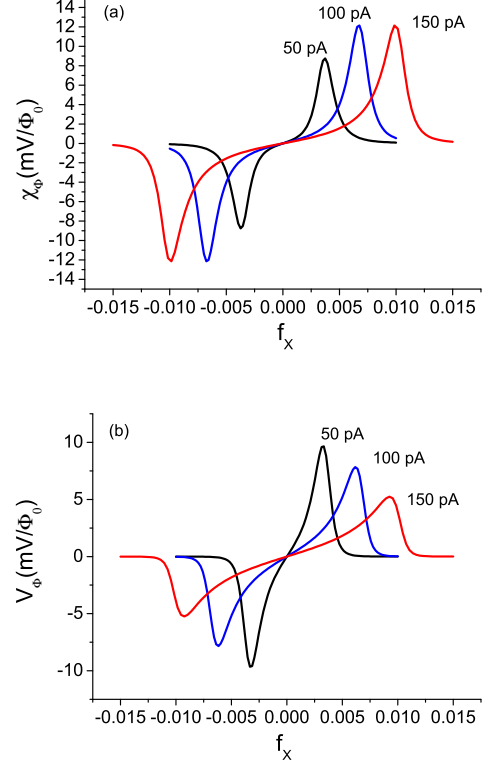


FIG. 3: (Color online). Phase-to-flux  $\chi_\Phi$  (a) and voltage-to-flux  $V_\Phi$  (b) transfer functions for three values of bias current  $I_0$ . The gap frequency  $\Delta/h = 2\text{GHz}$ .

$I_c = 400\text{ nA}$ , junction area  $A = 0.12\mu\text{m}^2$ ,  $T = 0.1\text{ K}$  we estimate for three-junction flux qubit (see Eq.18 in<sup>3</sup>)  $S_{\Phi, I_c}^{1/2} \approx 2 \times 10^{-8}\Phi_0/\text{Hz}^{1/2}$  at  $1\text{ Hz}$ . We will see that this value is almost one order of magnitude smaller than the noise from a preamplifier. Therefore, the self noise of the qubit can be neglected. The contribution of the voltage noise of the preamplifier to the flux resolution referred to the input is  $S_\Phi^V = S_V/V_\Phi^2$  or  $S_\Phi^V = S_V/\chi_\Phi^2$  depending on the detection mode. The current noise of preamplifier which is related to its noise temperature  $T_N$ ,  $S_I = 4k_B T_N/R_T$ , ( $R_T = \omega_T L_T Q$ ), contributes via two mechanisms. The first one comes from magnetic coupling between the tank inductance and the inductance of the qubit loop  $S_\Phi^I = M^2 Q^2 S_I$ . This contribution cannot be separated from the measured flux. The second mechanism contributes through a voltage noise induced by the current noise of the preamplifier across the dynamic resistance of the tank  $S_\Phi^D = R_D^2 S_I/V_\Phi^2$  (or  $S_\Phi^D = R_D^2 S_I/\chi_\Phi^2$ ), where  $R_D = \partial v/\partial I_0$ . By combining these three mechanisms we obtain for the flux sensitivity:

$$S_\Phi = M^2 Q^2 S_I + S_V/V_\Phi^2 + R_D^2 S_I/V_\Phi^2 \quad (5)$$

where  $R_D$  is approximately equal to  $R_T$ , the resistance of unloaded tank. In the case of the phase mode detection we should substitute in (5)  $\chi_\Phi$  for  $V_\Phi$ .

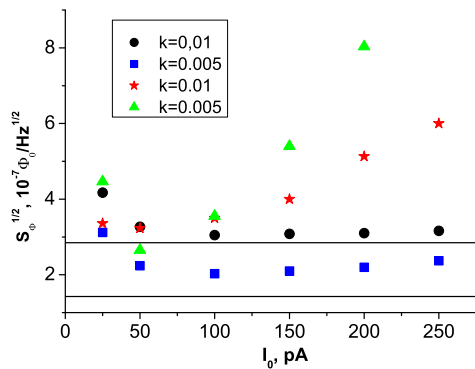


FIG. 4: (Color online). Flux sensitivity of qubit magnetometer. Phase detection mode is shown by boxes and circles. The stars and triangles are for the voltage detection. Two straight lines show the level of  $S_{\Phi,1}$  for  $k = 0.01$  (upper line) and  $k = 0.005$  (lower line).

For the estimation we take  $S_V^{1/2} = 0.2 \text{ nV/Hz}^{1/2}$ , and  $T_N = 0.1 \text{ K}$ <sup>11</sup>, with the other parameters being the same as for Figs. 2, 3. The inspection of Eq. (5) shows that the main contribution to the flux noise comes from the first term:

$$S_{\Phi,1} = M^2 Q^2 S_I = k^2 Q \frac{4k_B T_N L}{\omega_T} \quad (6)$$

This contribution does not depend on the position of the working point and for our parameters it gives  $S_{\Phi,1}^{1/2} = 2.8 \times 10^{-7} \Phi_0 / \text{Hz}^{1/2}$ . The influence of the last two terms

in Eq. (5) depends on the position of the working point and on the bias current amplitude  $I_0$ . In general, the contribution of these terms is nonnegligible. The total flux noise dependence on the amplitude of bias current is shown in Fig. 4. As seen from the figure phase detection in general is more favorable than voltage detection. It gives lower noise and is weakly sensitive to  $I_0$ . The flux resolution can be improved by a decrease of  $S_{\Phi,1}$  (see Eq. (6)) upon optimization of  $k$ ,  $Q$ ,  $\omega_T$ , or  $L$ . However, it does not necessarily lead to a decrease of the total noise, since the transfer functions also depend on these parameters. (See, for example, the  $k = 0.005$  curve in Fig. 4 for voltage detection). An increase of the bias frequency  $\omega_T$  can also give an improved flux resolution. However, for the qubit to remain in the ground state the condition  $\omega_T \ll \Delta/h$  should hold. We also made calculations for  $\omega_T = 200 \text{ MHz}$  with  $k=0.01$ ,  $Q=1000$ , with other parameters being unchanged. We obtain at  $I_0 = 200 \text{ pA}$  for the phase detection  $S_{\Phi}^{1/2} = 1.6 \times 10^{-7} \Phi_0 / \text{Hz}^{1/2}$ , which for  $L = 40 \text{ pH}$  corresponds to the energy sensitivity  $\varepsilon = S_{\Phi}/2L = 1.3 \times 10^{-33} \text{ J/Hz} = 2h$ . These values should be compared with those for conventional SQUIDS:  $S_{\Phi}^{1/2} \approx 10^{-6} \Phi_0 / \text{Hz}^{1/2}$ ,  $\varepsilon \approx 10^{-32} \text{ J/Hz}$ <sup>13</sup>.

In summary, we have shown that a superconducting flux qubit can be developed as a sensor of magnetic flux with an energy sensitivity close to the Planck constant.

We thank A. Izmalkov, M. Grajcar and D. Drung for fruitful discussions, and V. I. Shnyrkov for providing us with the manuscript of his paper prior to publication. E.I. thanks the EU for support through the RSFQubit and EuroSQIP projects. Ya. S. G. acknowledges the financial support from the ESF under grant No. 1030.

\* Electronic address: ilichev@ipht-jena.de

<sup>1</sup> Yu. Makhlin, G. Schön, and A. Shnirman, Rev. Mod. Phys. **73**, 357 (2001).

<sup>2</sup> O. Astafiev, Y. A. Pashkin, Y. Nakamura, T. Yamamoto, and J. S. Tsai, Phys. Rev. Lett. **93**, 267007 (2004).

<sup>3</sup> D. J. Van Harlingen, T. L. Robertson, B. L. T. Plourde, P. A. Reichardt, T. A. Crane, and John Clarke, Phys. Rev. B **70**, 064517 (2004).

<sup>4</sup> A similar idea has been considered in the work of V. I. Shnyrkov and S. I. Mel'nik (to be published in Fizika Nizkikh Temperatur (Low Temp. Phys.) 1, (2007), Kharkov, Ukraine). As distinct from our proposal, they studied a single junction interferometer with nonsinusoidal current phase relation. No estimations of the transfer functions or flux sensitivity were given.

<sup>5</sup> T.P. Orlando, J.E. Mooij, L. Tian, C.H. van der Wal, L. Levitov, S. Lloyd, and J.J. Mazo, Phys. Rev. B **60**, 15398 (1999).

<sup>6</sup> J.E. Mooij, T.P. Orlando, L. Levitov, L. Tian, C.H. van der Wal, and S. Lloyd, Science **285**, 1036 (1999).

<sup>7</sup> C.H. van der Wal, A.C.J. ter Haar, F.K. Wilhelm, R.N. Schouten, C.J.P.M. Harmans, T.P. Orlando, S. Lloyd, and

J.E. Mooij, Science **290**, 773 (2000).

<sup>8</sup> In principle, this condition can be sufficiently relaxed. In Ref. 9. it was shown that when the temperature was increased from  $T = 10 \text{ mK}$  to  $T = 200 \text{ mK}$  the width of the phase dip and therefore the steepness of the phase curve remained unchanged.

<sup>9</sup> Ya. S. Greenberg, A. Izmalkov, M. Grajcar, E. Il'ichev, W. Krech, H.-G. Meyer, M. H. S. Amin, and A. Maassen van den Brink, Phys. Rev. B **66**, 214525 (2002).

<sup>10</sup> M. Grajcar, A. Izmalkov, E. Il'ichev, Th. Wagner, N. Oukhanski, U. Hubner, T. May, I. Zhilyaev, H. E. Hoenig, Ya. S. Greenberg, V. I. Shnyrkov, D. Born, W. Krech, H.-G. Meyer, A. Maassen van den Brink, and M. H. S. Amin, Phys. Rev. B **69**, 060501(R) (2004).

<sup>11</sup> N. Oukhanski, M. Grajcar, E. Il'ichev, and H.-G. Meyer, Rev. Sci. Instr. **74**, 1145 (2003).

<sup>12</sup> D. Drung Supercond. Sci. Technol. **16**, 1320 (2003).

<sup>13</sup> *The SQUID Handbook*, edited by J. Clarke and A. I. Braginski, Fundamentals and Technology of SQUIDS and SQUID Systems (Wiley-VCH, Weinheim, 2004), Vol. I.